



Highly selective synthesis of triptycene *o*-quinone derivatives and their optical and electrochemical properties

Jian-Min Zhao^{a,b}, Hai-Yan Lu^b, Jing Cao^{a,b}, Yi Jiang^{a,b}, Chuan-Feng Chen^{a,*}

^aBeijing National Laboratory for Molecular Sciences, Center for Chemical Biology, Institute of Chemistry, Chinese Academy of Sciences, Beijing 100190, China

^bGraduate School, Chinese Academy of Sciences, Beijing 100049, China

ARTICLE INFO

Article history:

Received 8 September 2008

Revised 24 October 2008

Accepted 27 October 2008

Available online 31 October 2008

Keywords:

Triptycene *o*-quinone

Selective synthesis

Intramolecular CT interaction

Optical and electrochemical properties

DFT calculation

ABSTRACT

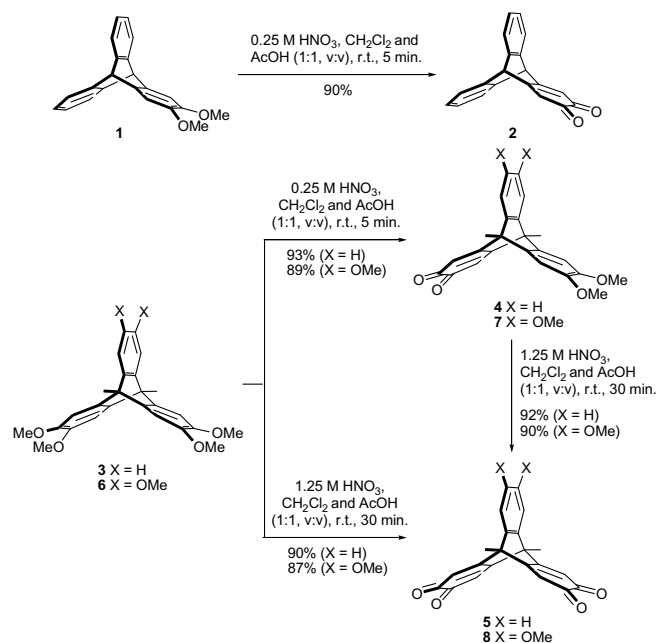
A convenient and efficient method for the selective synthesis of a series of triptycene *o*-quinone derivatives is described. The triptycene *o*-quinones, especially the ones containing the methoxy group(s) (electron donor) and the *o*-quinone group(s) (electron acceptor) simultaneously, show interesting intramolecular CT interactions and electrochemical properties. Moreover, DFT calculations display that introducing a strong electron-donor group into triptycene *o*-quinone results in an increasing of the HOMO energy level, which subsequently decreases the HOMO–LUMO energy gap.

© 2008 Elsevier Ltd. All rights reserved.

During the last decades, triptycene *p*-quinones¹ have attracted much attention for their unique 3D rigid frameworks, specific photochemical² and electrochemical properties,³ interesting chemical and biological activities,^{4,5} and wide applications in material sciences⁶ and supramolecular chemistry.⁷ Similarly, triptycene *o*-quinone derivatives are also a class of interesting compounds, but few are so far known.⁸ In this Letter, we report a convenient and efficient method for highly selective synthesis of a series of triptycene *o*-quinone derivatives, which show interesting optical and electrochemical properties studied by UV–vis spectra, cyclic voltammetry, and density functional theory (DFT) calculations. We believe that the triptycene *o*-quinones and their derivatives will find potential applications in wide research areas.

Synthesis of the triptycene *o*-quinone derivatives⁹ is depicted in Scheme 1. We first tested the reaction of *o*-dimethoxy-substituted triptycene **1** with dilute nitric acid (0.25 M) in CH₂Cl₂ and acetic acid (1:1, v:v) for several minutes, and the results showed that no nitration products were produced, but triptycene mono(*o*-quinone) **2** was selectively synthesized in 90% yield by an oxidation reaction. Under the same conditions as above, it was interesting to find that triptycene mono(*o*-quinone) **4** could be obtained as an orange solid in 93% yield by the selective oxidation of compound **3**. When the reaction was allowed to proceed for 1 h, compound **4** could be further oxidized by the dilute nitric acid to give triptycene bis(*o*-quinone) **5**. If 1.25 M nitric acid was used,

compound **5** could be directly obtained either from **3** in 90% yield or from **4** in 92% yield in 30 min.



Scheme 1. Synthesis of the triptycene *o*-quinone derivatives.

* Corresponding author. Tel.: +86 10 62588936; fax: +86 10 62554449.

E-mail address: cchen@iccas.ac.cn (C.-F. Chen).

Similarly, triptycene mono(*o*-quinone) **7** and triptycene bis(*o*-quinone) **8** could also be synthesized as dark red solids in high yields by treating compound **6** with nitric acid. When we tried to synthesize triptycene tri(*o*-quinone) (**9**) from the compound **6** according to the similar conditions as above, it did not succeed probably due to the lability of compound **9**. Moreover, it was found that both the triptycene mono(*o*-quinone)s **4** and **7** have good solubility in common polar and nonpolar solvents, but the triptycene bis(*o*-quinone)s **5** and **8** have low solubility in most solvents, except in DMSO.

The ^{13}C NMR spectra of **4** showed one signal at δ 180.2 for the two carbonyl carbons, eight signals for 16 aromatic carbons, and three signals for six aliphatic carbons, which indicates that it has a C_s symmetric structure. Similarly, the ^1H NMR and ^{13}C NMR spectra of compound **5** are consistent with its C_2 symmetric structure.



Figure 1. (a) Top view and (b) side view of crystal structure of compound **5**. The thermal ellipsoids were drawn at 50% probability level. Solvent molecules and hydrogen atoms were omitted for clarity.

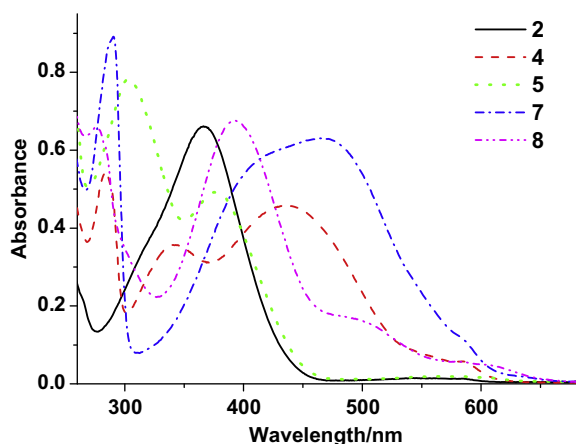


Figure 2. UV-vis absorption spectra of triptycene *o*-quinone derivatives in CH_2Cl_2 (0.1 mM).

The structure of **5** was further determined by its X-ray single-crystal analysis (Fig. 1).¹⁰ Moreover, we also found that **5** can be packed into a 3D microporous structure in the solid state, in which DMSO molecules are located in the channels.¹¹ For compounds **7** and **8**, their ^1H NMR spectra showed only four singlet signals, meanwhile their ^{13}C NMR spectra showed one signal for the carbonyl carbons, five signals for the aromatic carbons, one signal for the bridgehead carbons, and two signals for the methyl carbons, which are consistent with their C_2 symmetric structures.

The UV-vis absorption spectra of the triptycene *o*-quinones were carried out in CH_2Cl_2 . As shown in Figure 2, compound **4** exhibited a typical intramolecular charge-transfer (CT) band at 436 nm ($\log \epsilon$ 3.66), which might be attributed to the CT transition for the symmetry-forbidden CT interaction¹² between the electron donor (D) of the catechol unit and the electron acceptor (A) of *o*-benzoquinone unit fixed in the rigid framework. Similarly, the CT bands at 468 nm ($\log \epsilon$ 3.80) and 480 nm ($\log \epsilon$ 3.24) were also observed in the absorption spectra of compounds **7** and **8**, respectively, which displayed the successive red shifts by 32 nm and 44 nm, respectively, compared with the CT band of **4**. Moreover, the observations also suggested that the contribution of the triptycene *o*-quinone **7** with DAD-type nonparallel 3D structure to CT band strength is more than that of compound **8** with ADA-type 3D structure. In the cases of compounds **2** and **5**, no apparent CT bands but only characteristic absorption bands of the π - π^* and n - π^* transitions of the quinone moiety were observed, which might be due to the weak electron donor of the benzene ring.

We further evaluated the electrochemical properties of the triptycene *o*-quinones by cyclic voltammetry (CV) in CH_2Cl_2 with 0.1 M $n\text{-(NBu}_4\text{)PF}_6$ as the supporting electrolyte, and the results are summarized in Table 1. As shown in Figure 3, the CV curve of **4** exhibits one couple of well-defined cathodic and anodic peaks with the half-wave potential of -0.81 V, which is similar to those of the *o*-benzoquinones, and consistent with a two-electron redox process.¹³ For compound **5** with two *o*-quinone moieties, two couples of cathodic and anodic peaks, in which one couple of the peaks was almost the same as those of **4** while the other ones moved to less negative values ($E_{1/2} -0.54$ V), were observed. The results suggested that each of the *o*-quinone moieties in **5** shows a two-electron redox process, moreover, the second quinone unit is more easily reduced when compared with the first quinonoid ring. Similarly, both **2** and **7** also displayed a two-electron redox process, meanwhile two couples of cathodic and anodic peaks were observed for the *o*-quinone units in triptycene bis(*o*-quinone) **8**.¹¹

To gain insight into the electronic properties of triptycene *o*-quinones, we carried on DFT calculations to optimize the structure of triptycene *o*-quinones using the B3LYP functional and a 6-311G(d) basis set. All the calculations have been performed with GAUSSIAN 03 program package. The calculated frontier orbit energies,

Table 1
Summary of the physical property measurements of *o*-benzoquinone and triptycene *o*-quinones

Compound	λ_{CT} ($\log \epsilon$) nm (dm^3/mol)	$E_{1/2}/\text{V}$ ($\Delta E/\text{mV}$) ^a	E_g/eV ^b	HOMO/eV ^c	LUMO/eV ^d	HOMO/eV ^e	LUMO/eV ^e	Calcd E_g/eV ^e	Dipole moment/D ^e
<i>o</i> -Benzoquinone	—	—	—	—	—	-7.18	-4.00	3.18	5.81
2	—	-0.82 (290)	2.77	-6.60	-3.83	-6.77	-3.51	3.26	7.73
4	436 (3.66)	-0.81 (260)	2.07	-5.85	-3.78	-5.98	-3.35	2.63	8.17
5	—	-0.54 (250)	2.72	-6.78	-4.06	-7.15	-4.24	2.91	7.49
7	468 (3.80)	-0.85 (260)	2.03	-5.72	-3.69	-5.79	-3.24	2.55	8.47
8	480 (3.24)	-0.55 (220)	1.98	-6.01	-4.03	-6.45	-4.13	2.32	8.26
		-0.81 (220)							

^a Performed with a three-electrode system (platinum disk as working electrode, platinum rod as counter electrode, and Ag/Ag^+ as reference electrode) in CH_2Cl_2 containing 0.1 M $n\text{-Bu}_4\text{NPF}_6$ as a supporting electrolyte at a scan rate of 0.1 V s^{-1} .

^b Estimated from the onset of the absorption spectra ($E_g = 1240/\lambda_{\text{max}}$).

^c Calculated by $\text{HOMO} = \text{LUMO} - E_g$.

^d Calculated from the empirical formula: $\text{LUMO} = -(4.44 + E_{\text{onset}})$.

^e Obtained from the DFT/B3LYP calculation.

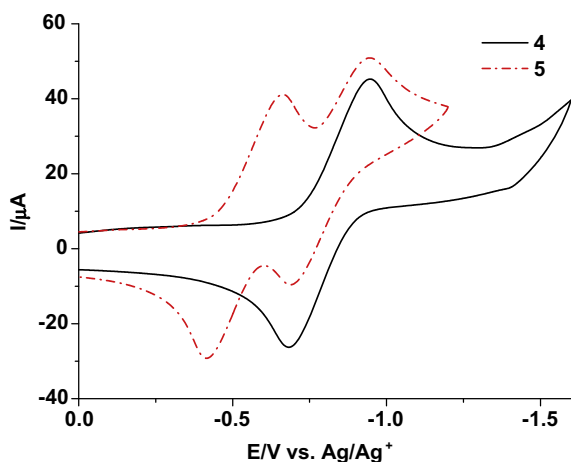


Figure 3. Cyclic voltammograms of compounds **3**, **4**, and **5** (5.0 mM) in CH_2Cl_2 with $n\text{-Bu}_4\text{NPF}_6$ (0.1 M) as the supporting electrolyte. Scan rate: 0.1 V s^{-1} .

energy gaps, and the corresponding dipole moments of triptycene *o*-quinones are summarized in Table 1. As shown in Figure 4, the frontier orbitals of **4** indicate that its HOMO is mainly located on the *o*-dimethoxy benzene ring, while the LUMO is concentrated mostly within the *o*-benzoquinone moiety. However, both the HOMO and LUMO of **5** are mainly concentrated within the two *o*-benzoquinone moieties. Similar distributions to **5** also exist in *o*-benzoquinone and triptycene mono(*o*-quinone) **2**.¹¹ The HOMO–LUMO energy gap of **4** was calculated to be 2.63 eV, which decreased by 0.55 eV and 0.63 eV, respectively, compared with those of *o*-benzoquinone and **2**. It was further found that compared with other triptycene *o*-quinones, compound **8** has lowest HOMO–LUMO energy gap (2.32 eV), which is consistent with its CT band in long wavelength region observed in the absorption spectrum. Thus, a conclusion can be drawn that introducing a strong electron-donor group into triptycene *o*-quinone results in an increasing of the HOMO energy level, which subsequently decreases the HOMO–LUMO energy gap. Moreover, the HOMO and LUMO energy levels of the triptycene quinones were also obtained using the onset of the first reduction process (E_{onset}) and the energy band gaps (E_g) (Table 1). The calculated HOMO/LUMO energy levels and energy gaps are within 0.45 and 0.56 eV of values determined by the UV spectra and electrochemistry, respectively. These offset may be attributed to irreversible redox process and charge-transfer character of triptycene quinones.

In summary, we have presented a convenient and efficient method for the selective synthesis of a series of triptycene *o*-quinone derivatives in high yields, and have further found that

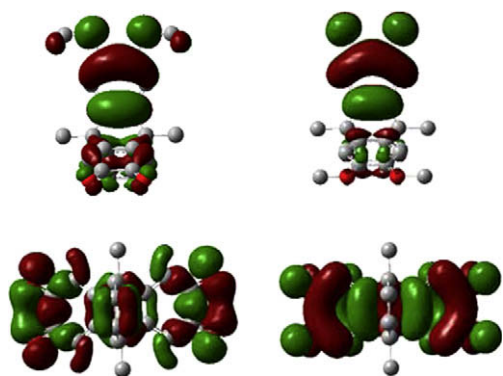


Figure 4. Frontier orbitals HOMO (left) and LUMO (right) of **4** (top) and **5** (bottom).

the triptycene *o*-quinones, especially the ones containing the methoxy group(s) (electron donor) and the *o*-quinone group(s) (electron acceptor) simultaneously, showed interesting intramolecular CT interactions and electrochemical properties. Moreover, DFT calculations further displayed that introducing a strong electron-donor group into triptycene *o*-quinone results in an increasing of the HOMO energy level, which subsequently decreases the HOMO–LUMO energy gap. We believe that the results presented here can provide a lot of opportunities to develop new supramolecular systems, and also find wide applications in the design and construction of new functional materials, which are underway in our laboratory.

Acknowledgments

We thank the National Natural Science Foundation of China (20532030, 20625206), National Basic Research Program (2007CB808004), and the Chinese Academy of Sciences for financial support. We also thank Dr. H. B. Song at Nankai University for determining the crystal structure.

Supplementary data

Supplementary data (cyclic voltammograms of triptycene *o*-quinones. Frontier orbitals of *o*-benzoquinone and triptycene *o*-quinones) associated with this article can be found in the online version, at doi:10.1016/j.tetlet.2008.10.128.

References and notes

- (a) Bartlett, P. D.; Ryan, M. J.; Cohen, S. G. *J. Am. Chem. Soc.* **1942**, *64*, 2649–2653; (b) Iwamura, H.; Makino, K. *J. Chem. Soc., Chem. Commun.* **1978**, 720–721; (c) Russel, G. A.; Suleman, N. K.; Iwamura, H.; Webster, O. W. *J. Am. Chem. Soc.* **1981**, *103*, 1560–1561; (d) Chen, C.-F.; Han, T.; Jiang, Y. *Chin. Sci. Bull.* **2007**, *52*, 1349–1361.
- (a) Tai, Y. F.; Janet, N.; Gamlin, G. O.; Scheffer, J. R.; Trotter, J.; Young, D. T. *Tetrahedron Lett.* **1995**, *36*, 2025–2028; (b) Borecka, B.; Gamlin, J. N.; Gudmundsdottir, A. D.; Olovsson, G.; Scheffer, J. R.; Trotter, J. *Tetrahedron Lett.* **1996**, *37*, 2121–2124; (c) Wiehe, A.; Senge, M. O.; Kurreck, H. *Liebigs Ann. Recl.* **1997**, 1951–1963; (d) Wiehe, A.; Senge, M. O.; Schäfer, A.; Speck, M.; Tannert, S.; Kurreck, H.; Röder, B. *Tetrahedron* **2001**, *57*, 10089–10110.
- Yamamura, K.; Miyake, H.; Himeno, S.; Inagaki, S.; Nakasujii, K.; Murata, I. *Chem. Lett.* **1988**, 1819–1822.
- (a) Hua, D. H.; Tamura, M.; Huang, X.; Stephany, H. A.; Helfrich, B. A.; Perchellet, E. M.; Sperflage, B. J.; Perchellet, J. P.; Jiang, S.; Kyle, D. E.; Chiang, P. K. *J. Org. Chem.* **2002**, *67*, 2907–2912; (b) Spyroudis, S.; Xanthopoulou, N. *J. Org. Chem.* **2002**, *67*, 4612–4614; (c) Spyroudis, S.; Xanthopoulou, N. *Tetrahedron Lett.* **2003**, *44*, 3767–3770; (d) Zhu, X.-Z.; Chen, C.-F. *J. Org. Chem.* **2005**, *70*, 917–924.
- Perchellet, E. M.; Magill, M. J.; Huang, X.; Brantis, C. E.; Hua, D. H.; Perchellet, J. P. *Anti-Cancer Drugs*. **1999**, *10*, 749–766.
- (a) Norvez, S.; Simon, J. *J. Chem. Soc., Chem. Commun.* **1990**, 1398–1399; (b) Norvez, S. *J. Org. Chem.* **1993**, *58*, 2414–2418; (c) Long, T. M.; Swager, T. M. *J. Am. Chem. Soc.* **2003**, *125*, 14113–14119.
- (a) Yang, J. S.; Liu, C. P.; Lin, B. C.; Tu, C. W.; Lee, G. H. *J. Org. Chem.* **2002**, *67*, 7343–7354; (b) Masao, H.; Kimiaki, Y.; Jun, Y. *Tetrahedron* **2001**, *57*, 10253–10258; (c) Scheib, S.; Cava, M. P.; Baldwin, J. W.; Metzger, R. M. *J. Org. Chem.* **1998**, *63*, 1198–1204; (d) Yang, J. S.; Yan, J. L. *Chem. Commun.* **2008**, 1501–1512.
- (a) Gong, K.-P.; Zhu, X.-Z.; Zhao, R.; Xiong, S.-X.; Mao, L.-Q.; Chen, C.-F. *Anal. Chem.* **2005**, *77*, 8158–8165; (b) Chong, J. H.; MacLachlan, M. J. *J. Org. Chem.* **2007**, *72*, 8683–8690.
- Compounds **1**,^{14a} **3**,^{14b} and **6**^{14c} were prepared according to the literature procedures. *Synthesis of 2*. To a solution of **1** (110 mg, 0.35 mmol) in CH_2Cl_2 and AcOH (1:1, 15 mL) was added 68% HNO_3 (0.25 mL) dropwise. After about 5 min, the reaction mixture was poured into cold water. The resulted mixture was partitioned by CH_2Cl_2 and water. The organic layer was washed with 10% NaHCO_3 solution and dried over anhydrous Na_2SO_4 . After removal of the solvent, the residue was subjected to column chromatography (silica gel, ethyl acetate/dichloromethane = 1:20 as eluent) to give the pure product **2**^{8a} (89 mg, 90%). *Synthesis of 4*. To a solution of **3** (450 mg, 1.12 mmol) in CH_2Cl_2 and HOAc (1:1, v/v, 30 mL) was added 68% HNO_3 (0.5 mL) dropwise. After about 5 min, the reaction mixture was then worked up as described above to give compound **4** (387 mg, 93%) as an orange solid. Mp 228–230 °C. $^1\text{H NMR}$ (300 MHz, CDCl_3): δ 7.37–7.40 (m, 2H), 7.28–7.31 (m, 2H), 6.90 (s, 2H), 6.22 (s, 2H), 3.90 (s, 6H), 2.23 (s, 6H). $^{13}\text{C NMR}$ (75 MHz, CDCl_3): δ 13.7, 46.7, 56.3, 105.8, 118.3, 121.5, 127.7, 133.8, 141.7, 148.9, 156.7, 180.2. IR (KBr, cm^{-1}): 1682.1, 1661.5. EI-MS: m/z 372 (M^+). Elemental Anal. Calcd for $\text{C}_{24}\text{H}_{20}\text{O}_4$: C, 77.40; H, 5.41. Found: C, 77.06; H, 5.61. *Synthesis of 5*. To a solution of **3** (422 mg, 1.05 mmol) or **4**

(781 mg, 2.10 mmol) in CH_2Cl_2 and HOAc (1:1, v/v, 30 mL) was added 68% HNO_3 (2.5 mL) dropwise. After 30 min, the reaction mixture was poured into cold water. The resulted mixture was partitioned by CH_2Cl_2 and water. The organic layer was washed with 10% NaHCO_3 solution and dried over anhydrous Na_2SO_4 . After removal of the solvent, the residue was subjected to column chromatography (silica gel, ethyl acetate/dichloromethane = 1:10 as eluent). The pure product **5** was obtained as a yellow solid (323 mg, 90% from **3** or 660 mg, 92% from **4**). Mp 264–266 °C (dec). ^1H NMR (300 MHz, $\text{DMSO}-d_6$): δ 7.47 (s, 4H), 6.39 (s, 4H), 2.00 (s, 6H). ^{13}C NMR (75 MHz, $\text{DMSO}-d_6$): δ 13.4, 46.2, 121.3, 122.5, 129.1, 137.8, 152.3, 178.9. IR (KBr, cm^{-1}): 1683.3, 1663.3. EI-MS: m/z 342 (M^+). Elemental Anal. Calcd for $\text{C}_{22}\text{H}_{14}\text{O}_4 \cdot 0.4\text{CH}_3\text{CO}_2\text{C}_2\text{H}_5$: C, 75.07; H, 4.59. Found: C, 75.09; H, 4.91. *Synthesis of 7*. Compound **7** was synthesized in 89% yield by the same method as that of **2** from compound **6**. Mp 238–239 °C. ^1H NMR (300 MHz, CDCl_3): δ 6.90 (s, 4H), 6.20 (s, 2H), 3.90 (s, 12H), 2.22 (s, 6H). ^{13}C NMR (75 MHz, CDCl_3): δ 13.9, 46.2, 56.3, 105.7, 117.7, 134.0, 148.9, 156.4, 180.4. IR (KBr, cm^{-1}): 1682.1, 1662.2. EI-MS: m/z 432 (M^+). Elemental Anal. Calcd for $\text{C}_{26}\text{H}_{24}\text{O}_6 \cdot 0.2\text{CH}_3\text{CO}_2\text{C}_2\text{H}_5$: C, 71.52; H, 5.73. Found: C, 71.93; H, 6.04. *Synthesis of 8*. Compound **8** (157 mg, 87% from **6** or 101 mg, 90% from **7**) was synthesized from compound **6** (210 mg, 0.45 mmol) or **7** (120 mg, 0.28 mmol) by the same method as that of compound **5**. Mp 254–256 °C (dec). ^1H NMR (300 MHz, $\text{DMSO}-d_6$): δ 6.98 (s, 2H), 6.35 (s, 4H), 3.82 (s, 6H), 1.97 (s, 6H). ^{13}C NMR (75 MHz, $\text{DMSO}-d_6$): δ 13.5, 45.8, 56.0, 106.9, 120.7, 129.6, 149.8, 152.6,

179.2. IR (KBr, cm^{-1}): 1685.8, 1666.1. EI-MS: m/z 402 (M^+). Elemental Anal. Calcd for $\text{C}_{24}\text{H}_{18}\text{O}_6 \cdot 0.5\text{CH}_3\text{CO}_2\text{C}_2\text{H}_5$: C, 69.95; H, 4.97. Found: C, 70.23; H, 5.06.

- X-ray crystal data for **5**. $\text{C}_{26}\text{H}_{26}\text{O}_2\text{S}_{12.5}$, $M_r = 771.22$, crystal size: $0.26 \times 0.24 \times 0.20 \text{ mm}^3$, orthorhombic, space group $Pnma$, $a = 16.354(3) \text{ \AA}$, $b = 15.222(3) \text{ \AA}$, $c = 9.4093(19) \text{ \AA}$, $\beta = 90.00^\circ$. $V = 2342.4(8) \text{ \AA}^3$, $Z = 4$, $T = 113(2) \text{ K}$. 27,381 reflections collected, 2893 independent ($R_{\text{int}} = 0.0463$), giving $R_1 = 0.0514$ for observed unique reflection [$I > 2\sigma(I)$] and $wR_2 = 0.1365$ for all data. CCDC 695101 contains the supplementary crystallographic data for **1a-2a**. The data can be obtained free of charge from The Cambridge Crystallographic Data Centre via www.ccdc.cam.ac.uk
- See Supplementary data.
- (a) Iwamura, H.; Makino, H. *J. Chem. Soc., Chem. Commun.* **1978**, 720–721; (b) Murata, I. *Pure Appl. Chem.* **1983**, 55, 323–330; (c) Yamamura, K.; Nakasuji, K.; Murata, I.; Inagaki, S. *J. Chem. Soc., Chem. Commun.* **1982**, 396–397; (d) Norvez, S.; Barzoukas, M. *Chem. Phys. Lett.* **1990**, 165, 41–44; (e) Nobuya, K. *Bull. Chem. Soc. Jpn.* **1989**, 62, 800–807.
- Chambers, J. Q. In *The Chemistry of the Quinonoid Compounds*; Patai, S., Ed.; Wiley: New York, 1974; pp 737–792.
- (a) Peng, X.-X.; Lu, H.-Y.; Han, T.; Chen, C.-F. *Org. Lett.* **2007**, 9, 895–898; (b) Zong, Q.-S.; Chen, C.-F. *Org. Lett.* **2006**, 8, 211–214; (c) Zhu, X.-Z.; Chen, C.-F. *J. Am. Chem. Soc.* **2005**, 127, 13158–13159.